CONSISTENT CORE-EDGE MODELLING OF IMPURITY-SEEDED DEMO PLASMA

G.W. Pacher[1], H.D. Pacher[2], A.S. Kukushkin[3], G. Janeschitz[3], V. Kotov[4], D. Reiter[4], D.P. Coster[5]
[1]Hydro-Québec, Varennes, Canada, [2]INRS-EMT, Varennes, Canada, [3]ITER Organization, Cadarache, France, [4]FZ Jülich, Jülich, Germany, [5]MPI für Plasmaphysik, Garching, Germany

The ICPS methodology to describe in a coherent way the entire plasma from the centre via the pedestal and the scrape-off layer to the divertor plate, which has been developed for ITER ([1], [2]), is applied here to impurity seeded scenarios in a prototypical DEMO geometry [3] in order to quantify the core impurity contamination associated with a given level of radiation and the effect on the pulse length. For DEMO modelling, the state of the art comprehensive nonlinear neutral model [4], [5] of the edge and divertor region provides the boundary conditions for the core. With the implementation of parallel processing for B2-EIRENE, it is now possible to simulate seeding with medium-Z impurity (neon), leading to scaling relationships for the key parameters in DEMO which are then used in DEMO core simulations as boundary conditions as in [1], [2] for ITER.

The key parameter for the edge plasma and the detachment state [4], [5] is $\mu \equiv p_{\mathrm{DT}\,\#}\, P_{\#}^{-0.87} f_{\mathrm{f}}^{-0.8} f_{\mathrm{w}}^{-1}\, q_{95\,\#}^{-0.27} f_{\mathrm{nn}}^{\;-1} R_{\#}^{-1.21}$, which is proportional to $p_{\mathrm{DT}\,\#}$, the normalised average neutral pressure at the divertor-PFR interface. The edge-based density limit is taken to occur at detachment of the inner divertor ($\mu = 1$), and its density analogue for the edge density is $f_{sat\_n} = \mu^{0.43}$.

As for ITER, the DT density increases with decreasing Ne seeding in DEMO for the same edge operating point (same normalized divertor pressure μ [4],[5], i.e. same detachment state) because more power is available for ionisation, but the detailed variation is different, probably due to profile effects (for ITER, n_{Ne_sep} in the scaling below was multiplied by 40). The scaling, shown in fig. 1 left, is given by:
$n_{\mathrm{DT\_sep}} + 20 n_{\mathrm{Ne\_sep}} = 0.53 f_f^{\;0.8} S_{\#}^{\;0.28} P_{\#}^{\;0.55} \xi_{ei}^{\;0.05} f_w^{\;0.68} f_q^{\;-0.5} R_{\#}^{\;1.02} \mu^{0.23}$ (for Ne-seeded DEMO) where $R_{\#}$ - normalised divertor radius, $P_{\#}$ - power into SOL normalised by $R_{\#}^3$, $q_{95\#}$ - normalised safety factor (normalisation and definitions of fuelling f_{f} , wall f_{w}, neutral model f_{nn} factors are given in [4]; $S_{\#}$ is the normalised DT pumping speed [6]).

On the whole, the previously established (with simpler neutral models) size scalings ([5] and references therein) hold, in particular the edge density limit. One difference, important in the present context, is that the impurity radiation and therefore the peak divertor power load (fig. 1 middle) do depend explicitly on neon density (this is not the case for ITER [5] because the trade-off between increased electron density and decreased Ne density in the radiation is different). The complete expression is (for $n_{Ne\_sep\_18}$ in [10^{18}m^{-3}]):

$$q_{pk} = 2.12 n_{Ne\_sep\_18}{}^{-0.6} f_f{}^{-0.6} S_\#{}^{0} P_\#{}^{1.26} \xi_{ei}{}^{0} f_w{}^{-0.37} f_q{}^{-0.5} R_\#{}^{-0.02} \mu^{-1.17} \quad \text{(for Ne-seeded DEMO)}$$

established for $0.5 < n_{Ne\_sep\_18} < 1$ and assumed to extrapolate to $0.4 < n_{Ne\_sep\_18} < 1.5$.

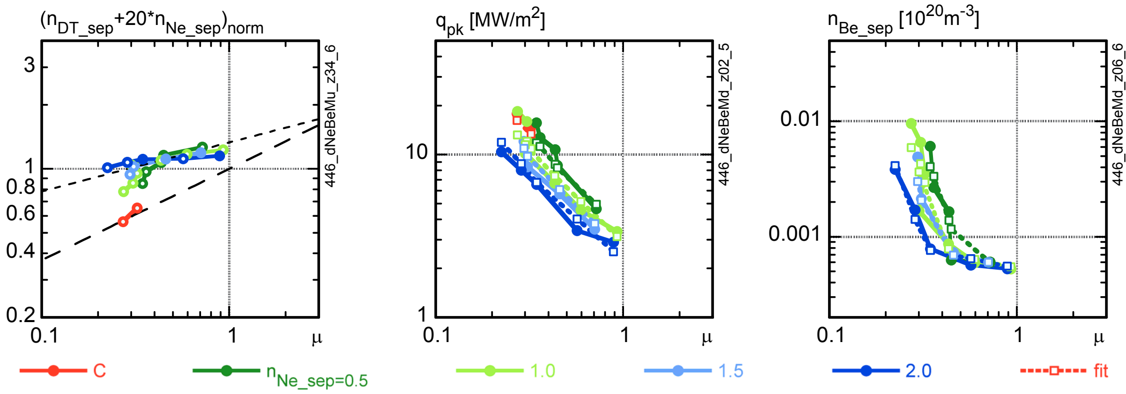

Fig. 1-Neon dependence of edge DT (left) and Be (right) densities and (centre) peak div. power load; hollow squares are the fits (the legend indicates $n_{\_Ne\_sep}$ in [10^{18}m^{-3}])

A new feature of the present DEMO simulations is the inclusion of sputtered beryllium from the walls (the divertor plates are assumed to be metallic, but not to erode significantly in almost detached operation) as an intrinsic impurity. It was found that beryllium erosion by neon increases very strongly toward low alpha powers (low densities far from detachment) but is unimportant for DEMO for the most interesting conditions of high power and long burn time (fig. 1 right - the base level is due to sputtering by DT). The resulting scaling expression is, limited to the maximum simulated value (minimum simulated Ne density):

$$n_{Be\_sep} = 5.37.10^{-4} \bullet \max\left[\mu^{-0.33}, 0.018 n_{Ne\_sep\_18}{}^{-2.1} \mu^{-4.15}\right] \text{ for } \mu > 0.2$$

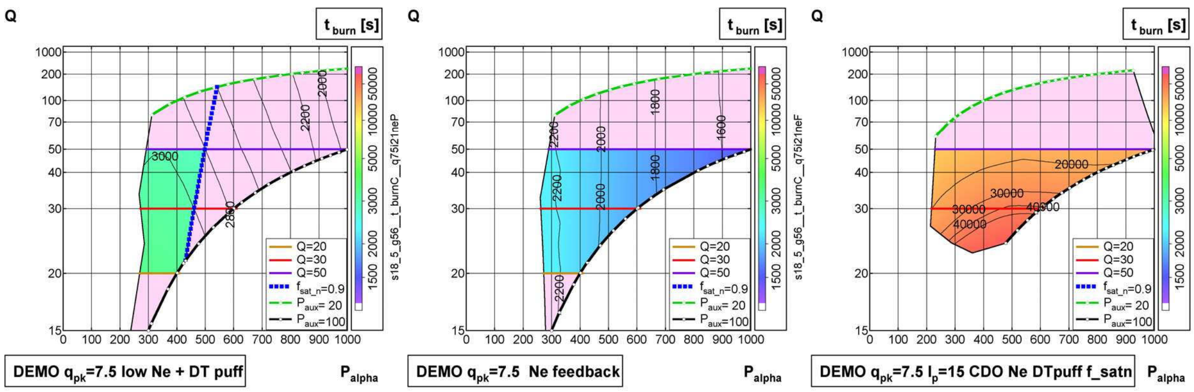

Fig. 2-Burn duration for (left to right) scenarios A, B, and H of Table I. Dashed blue line f_sat_n=0.9, operating space (coloured) between Q=20 & 50, red line Q=30

Core simulations were performed to trace out the operational space of DEMO in partially attached ELMy H-mode operation (condition $f_{sat\_n} \leq 0.9$, i.e. $\mu \leq 0.78$) in the manner and with the model described in detail in [2]. As in [3], the region relevant for DEMO operation is defined as $20 \leq Q \leq 50$, with a typical value of Q=30. Operating diagrams of burn duration plotted in the Q-P_α plane (suitable for performance evaluation) are shown in fig. 2 for three representative cases assuming 100 Vs available for burn at 21 MA.

	A	B	C	D	E	F	G	H
I	21	21	21	18	18	18	18	15
cd	n	n	y	y	y	y	y	y
F_α	1	1	1	1	1.5	2	2	2
puff	X			X	X	X		
Neon	min	X	X	min	max	max	V	V
f_{sat_n}	lim.			lim.			X	X

Table I. Conditions for each of the scenarios: "X" is the principal quantity which is varied to control the divertor power load, "min" and "max" are self-explanatory, "lim" indicates that the density limit is attained.d " V" indicates additional control by neon seeding when the limit is attained. Shading indicates change from previous scenario.

Scenario A (fig. 2 left) is for minimum neon concentration with divertor heat load controlled (q_{pk}≤7.8 MW/m^2) only by gas puff and in the absence of current drive. The edge-based density limit ([4], [5]) constrains operation in both power and burn time. In scenario B (middle) the divertor heat load is controlled by neon seeding alone without gas puff. The maximum accessible power then increases, but this is accompanied by a strong decrease in burn duration due to lower T_e and higher Z_{eff}. The "optimal" scenario H (Fig. 2 right, lower Q's than shown were not calculated) is that for which the divertor heat load is controlled by gas puff up to the edge density limit, and by additional impurity seeding only when this is not sufficient. For this case, current drive, as $j_{CD} = 0.2 \bullet 2\pi \bullet p \bullet (T/n_e)\ \left[MA/m^2, MW/m^3, 10keV, 10^{20}/m^3\right]$, is also operational. Finally, an improvement in confinement is postulated, corresponding to an enhancement factor of 2.0 on ballooning stability in the pedestal, similar to JET discharges (see [2]), which gives a confinement improvement of ~20% in DEMO. This allows the plasma current to be lowered to 15MA from the previous 21MA, which doubles the available flux for burn. Table I shows the progression of the scenarios from base to optimised.

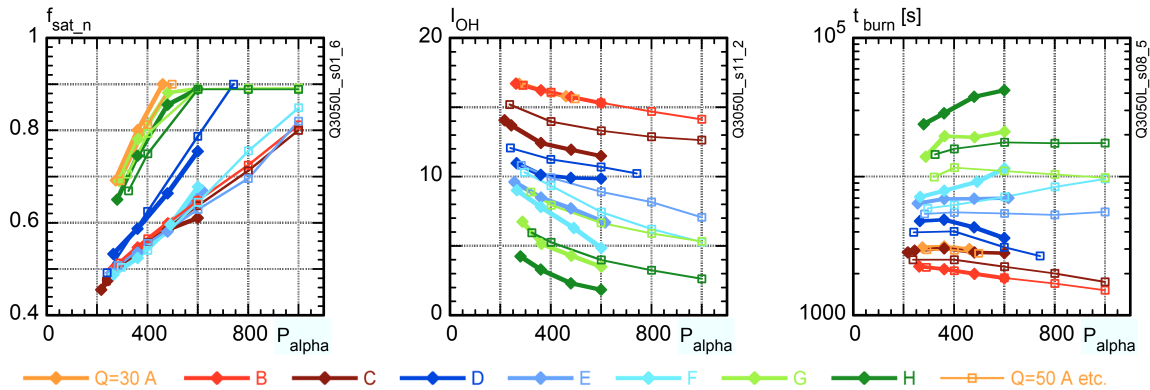

Fig. 3-Detachment $f_{\mathrm{sat\_n}}$, I_{OH}, and burn time for scenarios of Table I for Q=30 and 50 (same colours)

For the scenarios of Table I, important parameters are plotted on fig. 3 as a function of

P_α for both Q=30 (thick lines) and Q=50 (thin lines), showing on the left how f_{sat_n} rises for the purely impurity-seeded scenarios and is always high for the optimal scenarios with DT puffing which are seeded only as necessary. Fig. 3 centre shows the decrease of remaining inductively-driven current as current drive is applied, I_p is reduced to 18 MA, confinement is increased, and I_p is then further reduced to 15 MA. Fig. 4 shows the progression of the scenarios for $P_{aux} = 100$ MW (except when limited by f_{sat_n}) for Q=30 (P_α=600 MW) and Q=50, i.e. the end points of Fig. 3. At the same power, Q=50 needs higher n, giving lower T and average T/n and thus lower I_{CD} (but higher I_{BS}). I_{OH} is similar but loop voltage is higher and burn time lower for Q=50. The burn duration is seen to rise (Fig. 3 right, Fig. 4 bottom) progressively with the scenarios from ~2000s through ~4000s at 18 MA, standard confinement, to ~20,000s at 18 MA, improved confinement and optimised DT puff with Ne seed. For this optimised scenario, it was then possible to drop the current further, to 15 MA (from the original 21) and obtain a further increase in burn time. The non-inductive current fraction was then 85%, and the burn time was 20 times the original value, 40,000s.

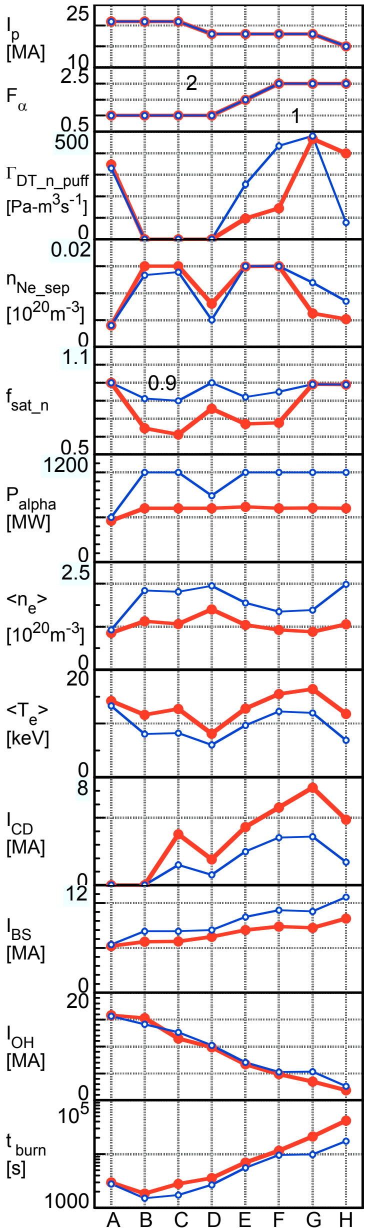

Fig. 4 - Parameters for different scenarios at Q=30 (red) and Q=50 (blue)

Our analysis has therefore demonstrated good results for DEMO with impurity seeding, with one-half day of burn (40,000 s) at 3 GW of fusion power and Q=30, close to reactor-like operation and not too far from steady state with the peak divertor power load at or below 7.8 MW/m^2. Performance improvements might come from choosing a higher-Z seed impurity (which can not presently be simulated for DEMO because of very slow convergence with multiple charge states), more advanced operation with yet better confinement, or from modifying the device geometry in order to increase the bootstrap current contribution.

[1] Pacher, G.W., Pacher, H.D., Janeschitz, G., Kukushkin, A.S., et al, Nucl. Fusion **47** (2007) 469
[2] Pacher, G.W., Pacher, H.D., Janeschitz, G., Kukushkin, A.S., et al, Nucl. Fusion **48** (2008) 105003
[3] Pacher, G.W., Pacher, H.D., Janeschitz, G., Kukushkin, A.S., et al, Proc. 22nd IAEA Fusion Energy Conf. Geneva (2008), paper IAEA-CN-165/IT/P6-15
[4] Pacher, H.D., Kukushkin, A.S., Pacher, G.W., Janeschitz, G., et al, J. Nucl. Mater. **363–365** (2007) 400
[5] Pacher, H.D., Kukushkin, A.S., Pacher, G.W., Kotov, V., et al, J. Nucl. Mater. **390–391** (2009) 259
[6] A.S. Kukushkin, H.D. Pacher, V. Kotov, et al., J. Nucl. Mater. **363-365** (2007) 308.